Journal Name

ARTICLE

# Pyridylphosphinate Metal Complexes: Synthesis, Structural Characterisation and Biological Activity

Received 00th January 20xx,
Accepted 00th January 20xx

DOI: 10.1039/x0xx00000x

www.rsc.org/

Jasmine M. Cross,[a] Natalie Gallagher,[b] Jason H. Gill,[b] Mohit Jain,[b] Archibald W. McNeillis,[a] Kimberly L. Rockley,[b] Fiona H. Tscherny,[a] Natasha J. Wirszycz,[a] Dmitry S. Yufit,[a] and James W. Walton[a]*

For the first time, a series of 25 pseudo-octahedral pyridylphosphinate metal complexes (Ru, Os, Rh, Ir) has been synthesised and assessed in biological systems. Each metal complex incorporates a pyridylphosphinate ligand, a monodentate halide and a capping $\eta^6$-bound aromatic ligand. Solid- and solution-state analyses of two complexes reveal a structural preference for one of a possible two diastereomers. The metal chlorides hydrolyse rapidly in $D_2O$ to form a 1:1 equilibrium ratio between the aqua and chloride adducts. The p$K_a$ of the aqua adduct depends upon the pyridyl substituent and the metal but has little dependence upon the phosphinate R' group. Toxicity was measured *in vitro* against non-small cell lung carcinoma H460 cells, with the most potent complexes reporting $IC_{50}$ values around 50 μM. Binding studies with selected amino acids and nucleobases provide a rationale for the variation in toxicity observed within the series. Finally, an investigation into the ability of the chelating amino acid L-His to displace the phosphinate O–metal bond shows the potential for phosphinate complexes to act as prodrugs that can be activated in the intracellular environment.

## Introduction

In the field of bioinorganic chemistry, platinum group metal complexes have found application in cellular imaging,[1] in enzyme inhibition[2] and as molecular probes of biological activity.[3] The therapeutic anticancer activity these complexes is also often probed both *in vitro* and *in vivo*.[4] In the context of therapeutics, the advantages that metal complexes offer over purely organic species include: a variety of metal geometries and coordination numbers, allowing access to intricate 3-dimensional structures; numerous metal oxidation states, allowing redox-activated drugs; tuneable ligands to vary sterics and electronics about the metal centre; exchangeable ligands, for *in situ* activation and binding to biomolecules; simple and modular syntheses, allowing rapid determination of structure to activity relationships. Despite the wide-spread clinical use of the platinum-based drugs, cisplatin, oxaliplatin and carboplatin,[5] there remains issues associated with side-effects, including dose-limiting systemic toxicities[6] and acquisition of drug resistance, which reduce the efficacy and clinical utility of these drugs.[7]

One class of metal complexes that has shown great promise as alternatives to Pt drugs are the pseudo-octahedral piano stool complexes,[8] in which a low-spin $d^6$ metal ion is capped by an $\eta^6$-phenyl or $\eta^5$-cyclopentadienyl ligand, with the remaining 3 coordination sites occupied by tri- bi- or mono-dentate ligands.

Over the past decades, many examples of piano stool metal complexes have been reported that show excellent *in vitro*[9] and *in vivo*[10] activity against cancers (Figure 1). Variation of each component of the piano stool arrangement alters the activity of the complex. For example, in the series $[(\eta^6\text{-arene})Ru(en)Cl]PF_6$ a 3-fold increase in activity against human ovarian cancer cell line A2780 is observed when the arene is varied from benzene to biphenyl.[11] Similarly, modulation of the mono-dentate halide in the series $[(\eta^6\text{-}p\text{-cym})Ru(p\text{-Azpy-NMe}_2)X]PF_6$ from chloride to iodide results in a decrease in $IC_{50}$, the concentration of complex required to inhibit cell proliferation by 50%, from 13 μM to 0.69 μM in the A2780 cell line.[12] Finally, complexes with the same ligand can vary in activity, depending upon the central metal. In the $[(\eta^6\text{-}p\text{-cym})M(picolinate)Cl]$ series, $IC_{50}$ values (A2780 cell line) of 45 μM[13] and 4.5 μM[14] were reported for the Ru and Os complexes, respectively. Beyond Ru(II) and Os(II), there are also a host of Ir(III) and Rh(III) piano-stool complexes, whose activity often surpasses that of related Ru(II) complexes.[15] Although often not well understood, the mechanism of action of these complexes may involve DNA binding,[16] interactions with histone proteins,[17] redox modulation[18] or enzyme inhibition.[19]

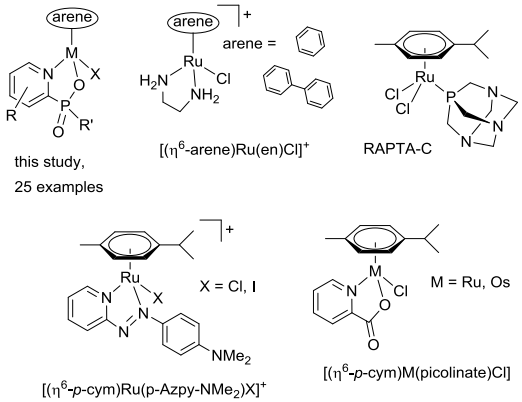


**Fig. 1** Examples of metal complexes assessed for their anticancer activity.

[a] *Department of Chemistry, Durham University, South Road, Durham, DH1 3LE, United Kingdom.*
[b] *School of Medicine, Pharmacy and Health, Durham University, Wolfson Research Institute, Queen's Campus, Stockton on Tees, TS17 6BH, United Kingdom.*

†Electronic Supplementary Information (ESI) available, includes full experimental procedures and X-ray structural data. See DOI: 10.1039/x0xx00000x

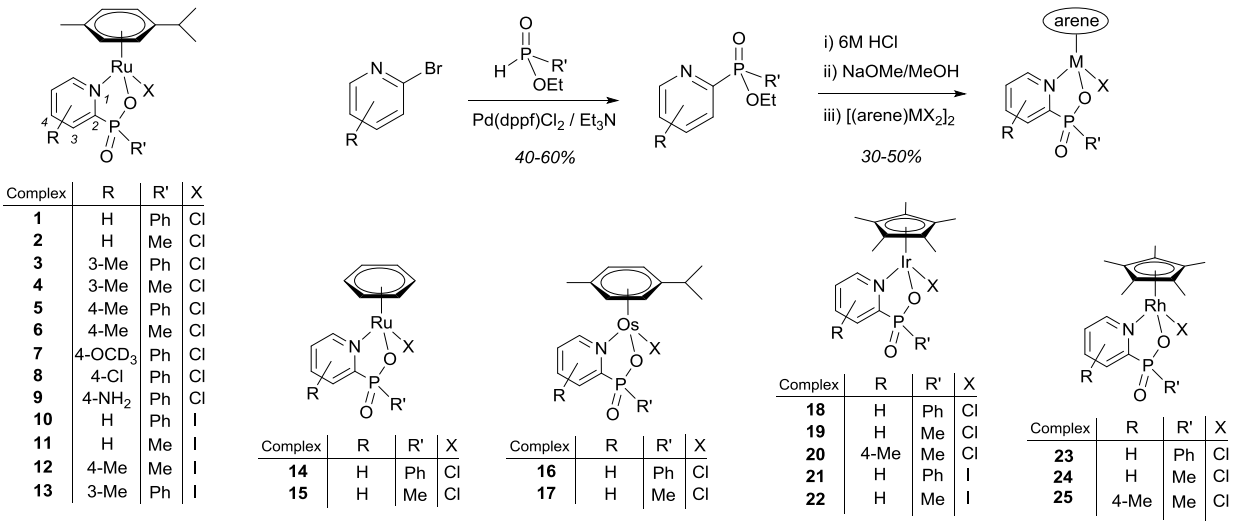


| Complex | R | R' | X |
|---|---|---|---|
| **1** | H | Ph | Cl |
| **2** | H | Me | Cl |
| **3** | 3-Me | Ph | Cl |
| **4** | 3-Me | Me | Cl |
| **5** | 4-Me | Ph | Cl |
| **6** | 4-Me | Me | Cl |
| **7** | 4-$OCD_3$ | Ph | Cl |
| **8** | 4-Cl | Ph | Cl |
| **9** | 4-$NH_2$ | Ph | Cl |
| **10** | H | Ph | I |
| **11** | H | Me | I |
| **12** | 4-Me | Me | I |
| **13** | 3-Me | Ph | I |

| Complex | R | R' | X |
|---|---|---|---|
| **14** | H | Ph | Cl |
| **15** | H | Me | Cl |

| Complex | R | R' | X |
|---|---|---|---|
| **16** | H | Ph | Cl |
| **17** | H | Me | Cl |

| Complex | R | R' | X |
|---|---|---|---|
| **18** | H | Ph | Cl |
| **19** | H | Me | Cl |
| **20** | 4-Me | Me | Cl |
| **21** | H | Ph | I |
| **22** | H | Me | I |

| Complex | R | R' | X |
|---|---|---|---|
| **23** | H | Ph | Cl |
| **24** | H | Me | Cl |
| **25** | 4-Me | Me | Cl |

**Scheme 1** General synthetic pathway and list of new complexes

The vast majority of reported piano stool complexes in the bioinorganic chemistry field incorporate polypyridyl, carboxylate or halide ligands. Only rarely are ligands explored that include elements other than C, N and O. However, there are a host of alternatives that may offer significant advantages over the more traditional ligand systems. In this study we present a novel ligand for platinum group metal complexes: the pyridylphosphinates. We report the synthesis, structural characterisation, aqueous properties and biological activities, including *in vitro* cytotoxicities, of a series of piano stool metal complexes incorporating the pyridylphosphinate ligand (Figure 1). Lanthanide complexes incorporating this ligand have found application in cellular imaging.[20] However, the piano stool pyridylphosphinate complexes have never been studied. Advantages of the pyridylphosphinate ligand include: biocompatibility; the presence of a $^{31}$P-NMR spectroscopic handle; control over lipophilicity at phosphorus; modular synthesis allowing rapid structure-activity relationship profile and, finally, the presence a stereogenic phosphorus, which presents an opportunity to develop enantiomerically pure metal-based complexes.[21]

Despite the host of piano stool complexes that have been reported, there is often a lack of information on biological behaviour, such as interactions between biologically relevant molecules (amino acids, proteins and nucleobases) and the metal complexes. This information is needed as the changes in structure of the complexes that take place in the cellular environment will have a profound effect upon the biological activity. Herein, we interrogate the behaviour of the novel pyridylphosphinate complexes in biological systems, by monitoring metal-halide hydrolysis, measuring p$K_a$ values of the resultant aqua complexes and carrying out detailed binding studies with selected biomolecules.

## Synthesis and Structural Characterisation

A series of complexes were synthesised in order to assess the factors that determine aqueous biological behaviour. Systematic variation in the metal–arene combination, the metal-bound halide, the phosphorus R' group and the pyridyl R group led to a library of 25 new compounds (Scheme 1). Synthesis involves Pd-catalysed coupling of the phosphinate (HPO(OEt)R') and bromo-pyridyl precursors.[22] Quantitative hydrolysis of the phosphinate ester was followed by neutralisation with NaOMe and complexation with the appropriate metal dimer $[(arene)MX_2]_2$. Purification by recrystallisation from $CHCl_3/Et_2O$ gave the final complexes with 30-50% yields.[†]

The synthesis of complexes **7** and **8** (Scheme 2) proceeds via the 4-fluoropyridylphosphinate intermediate **L1**, which undergoes nucleophilic aromatic substitution to form the electron-rich 4-$OCD_3$- or electron-poor 4-Cl-pyridylphosphinate ligand, depending upon hydrolysis conditions.

Single crystals suitable for X-ray diffraction studies were grown of complexes **3** and **20** (Figures 2A and 3). Complex **3** crystallises in the monoclinic crystal system and the $P2_1/c$ space group and displays the expected pseudo-tetrahedral geometry, with the $\eta^6$-p-cymene occupying one vertex. Ru–Cl (2.4155(6) Å), Ru–O (2.0809(14) Å) and Ru–N (2.1109(17) Å) bond lengths are almost identical to those reported for the analogous picolinate complex [($\eta^6$-*p*-cym)Ru(picolinate)Cl],[13] however, the N–Ru–O bite angle is slightly larger in complex **3**, at 80.50(6)° (bite angle in picolinate complex is 77.95(7)°), reflecting the larger size of the phosphinate group. Intriguingly, of the four possible stereoisomers (*R* or *S* at Ru and P, denoted $Ru_{R/S}$ and $P_{R/S}$, respectively), only one enantiomeric pair is observed in the solid state structure – $Ru_SP_R$ and $Ru_RP_S$. $^1$H-NMR indicates that a single diastereomer is also present in solution, evidenced by one set of diastereotopic *p*-cymene protons in the region 5 – 6 ppm (Figure 2B). The origin of this stereoselectivity, which has also been observed in lanthanide pyridylphosphinate complexes,[23] can be rationalised in terms of the steric interactions between the *p*–cymene ligand and the P-phenyl group, which are

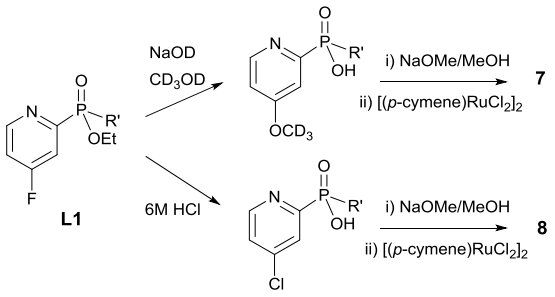


**Scheme 2**

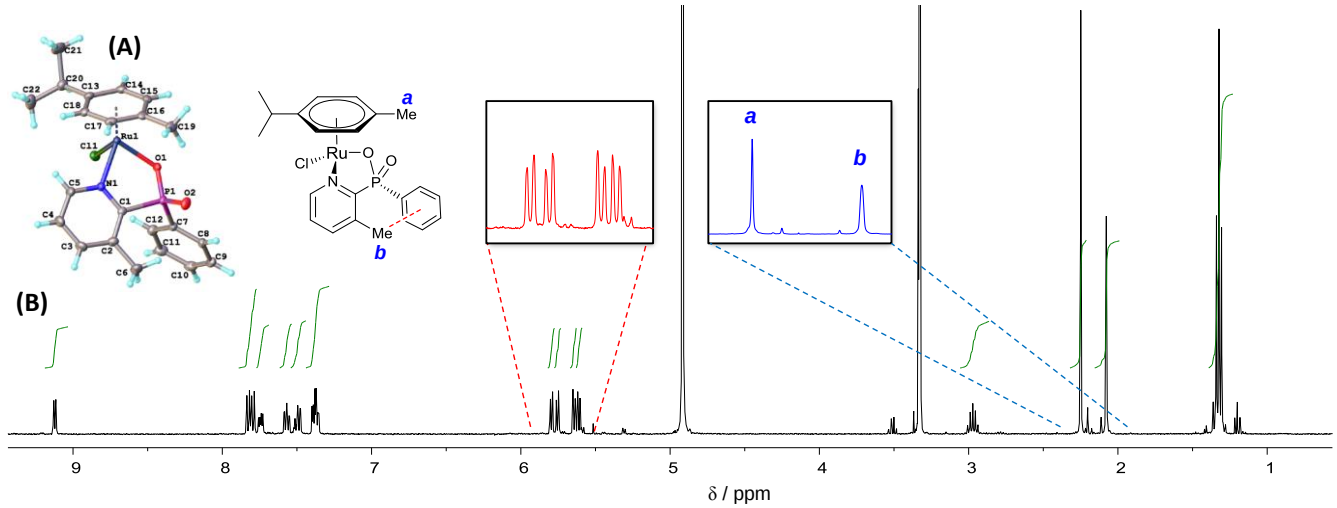


**Fig 2** (A) X-ray crystal structure of complex **3** and (B) $^{1}$H-NMR spectrum ($CD_3OD$, 298 K, 400 MHz,), with expansions of the single set of diastereotopic *p*-cymene protons and of the two methyl groups.

minimised in the observed diastereomer. Weak intramolecular hydrogen bonds between the P=O and p-cymene methyl-H (2.587 Å) and the P-phenyl and pyridyl methyl-H (3.065 Å) may also influence the observed stereochemistry. In solution, slight broadening of the pyridyl Me peak reflects its proximity to the P-phenyl aromatic system, but the presence of a sharp singlet peak for the p-cymene Me group suggests free rotation of the p-cymene ligand, as is expected for $\eta^6$-arene–metal bonds.[24]

The solid state structure of the Cp*-Ir complex **20** (Figure 3) shows several differences from complex **3**, including a Cc space group, longer bond lengths between the central metal and coordinated ligands and a wider N–metal–O bite angle of 82.00(11)°. Despite the presence of the less sterically challenging P-methyl phosphinate ligand, once again only a single diastereoisomer is observed – $Ir_SP_R$ and $Ir_RP_S$. No intramolecular H-bond interactions can be observed in the crystal structure, which presents further questions over the origin of this stereoselectivity. It may be that stereoselectivity originates from the initial attack of the phosphinate ligand on the metal dimer, during the formation of the complex.

## Aqueous Behaviour of the Complexes

To gain an understanding of the intracellular behaviour of metal complexes with biological application, it is essential to have an appreciation of the aqueous behaviour of new compounds. Upon dissolving complex **1** in a $D_2O$ : $CD_3OD$ (9 : 1) mix, equilibrium is established between the chloride (complex **1**) and aqua (complex **1a**) species (Figure 4). $^{1}$H-NMR of the *p*-cymene protons indicates that an approximate 1 : 1 (chloride : aqua) equilibrium is reached within 5 min and does not shift over the course of 24 h (Figure 4A). To confirm that the observed species are the chloride and aqua adducts, the complex was dissolved in 100 mM NaCl (Figure 4B) and in aqueous $AgNO_3$, followed by filtration of AgCl (Figure 4C), leading to the selective formation of the chloride and aqua adducts, respectively, each showing a characteristic set of diastereotopic protons. The analogous Ru-iodide complex also undergoes rapid hydrolysis with around 60% of the complex remaining as the intact iodide species.

At the extracellular chloride concentration (approx. 100 mM), the pyridylphosphinate complexes remains intact as the chloride adduct, but at lower intracellular chloride concentration (approx. 20 mM in cytoplasm)[25] significant amounts of the aqua adduct are present. With this in mind, we sought to measure the p$K_a$ of the bound water molecule and to establish how the p$K_a$ varies with the

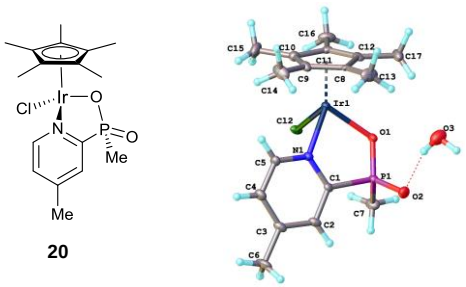


**20**



**Fig 3**. X-ray crystal structures of Ir complex **20.**

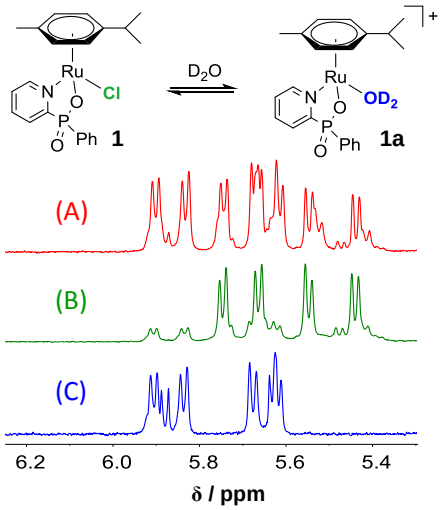


**Fig 4** $^{1}$H-NMR spectra ($D_2O$ : $CD_3OD$ 9:1, 298 K, 400 MHz) of (A) complex **1** and **1a** at approximately 1:1 equilibrium ratio, (B) chloride complex **1**, following addition of 100 mM NaCl and (C) aqua complex **1a**, following addition of $AgNO_3$ and filtration of AgCl.

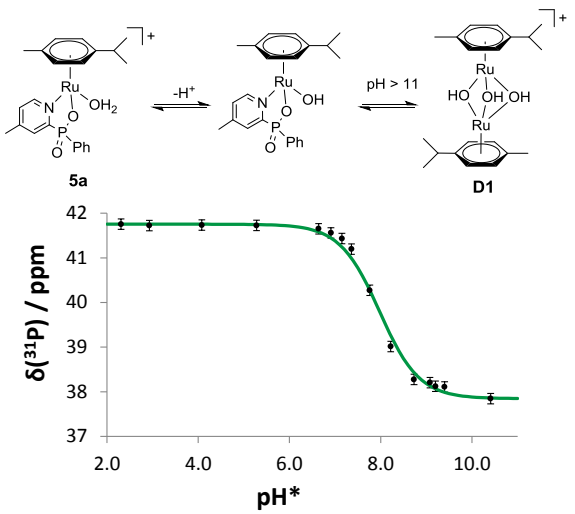


**Fig 5** Measurement of the p$K_a$* of aqua complex **5a** by monitoring the $^{31}$P-NMR spectrum ($D_2O$ : $CD_3OD$ 9:1, 298 K, 162 MHz) as a function of pH*. For Ru complexes, at approx. pH* > 11 formation of the hydroxy-bridged dimer **D1** is observed.

choice of central metal and coordinated ligands. p$K_a$* (p$K_a$ measured in $D_2O$) values were measured by monitoring the $^{31}$P- and $^1$H-NMR spectra of selected aqua complexes in $D_2O$ : $CD_3OD$ (9 : 1) as a function of pH* (pH values in $D_2O$ solution, Figure 5), according to established procedures[25] (see ESI† for full details). p$K_a$* values were converted to p$K_a$ values using the equation p$K_a$ = 0.929p$K_a$* + 0.42.[26] By comparing p$K_a$ values of selected aqua complexes (Table 1), it is apparent that a more electron donating pyridyl ligand leads to a higher p$K_a$. This is shown by the increase in values in the order **5a** < **3a** < **7a** for complexes with 4-Me, 3-Me and $OCD_3$ pyridyl substituents, respectively. This order reflects the higher pH required to deprotonate $H_2O$ bound to a more electron-rich metal centre. The phosphorus-bound R' group has little effect on p$K_a$, as can be seen by comparing values for **3a** and **4a**. Finally, as expected, the p$K_a$ value for the Ir complex **20a** is lower than that of the equivalent Rh complex **25a**, reflecting the increased metal–oxygen bond strength of the heavier congener.[27] For each of the studied Ru complexes, the hydroxyl-bridged dimer **D1** (Figure 5) forms at strongly basic pH (typically >pH 11), with concomitant loss of the pyridylphosphinate ligand.† The formation of this dimeric species from Ru piano stool complexes at elevated pH has been observed previously and the dimer is known to be non-cytotoxic.[28] NMR experiments indicate that dimer formation is partially reversible upon lowering the pH, but that complete regeneration of the starting complex does not take place.

**Table 1** p$K_a$ values for selected aqua complexes ($D_2O$ : $CD_3OD$ 9:1, 298 K). p$K_a$* values were measured by monitoring changes in $^{31}$P-NMR and $^1$H-NMR spectra and converted to p$K_a$ using the equation p$K_a$ = 0.929p$K_a$* + 0.42.[26]

| Complex | R | R' | {M(arene)} | p$K_a$ |
|---|---|---|---|---|
| **3a** | 3-Me | Ph | {Ru(p-cymene)} | 9.34 ± 0.04 |
| **4a** | 3-Me | Me | {Ru(p-cymene)} | 9.18 ± 0.19 |
| **5a** | 4-Me | Ph | {Ru(p-cymene)} | 7.76 ± 0.13 |
| **7a** | 4-$OCD_3$ | Ph | {Ru(p-cymene)} | 10.08 ± 0.05 |
| **20a** | 4-Me | Me | {Ir(Cp*)} | 9.31 ± 0.07 |
| **25a** | 4-Me | Me | {Rh(Cp*)} | 10.95 ± 0.04 |

**Table 2** $IC_{50}$ values for selected complexes measured using the MTT assay (72 h) against the non-small cell lung carcinoma H460 cell line. Entries are the mean value for data from at least three experiments. Complexes not included were found to have $IC_{50}$ > 200 μM

| Complex | R | R' | M | arene | X | $IC_{50}$ / μM |
|---|---|---|---|---|---|---|
| **1** | H | Ph | Ru | cym | Cl | >200 |
| **10** | H | Ph | Ru | cym | I | 65 ± 12 |
| **11** | H | Me | Ru | cym | I | >200 |
| **18** | H | Ph | Ir | Cp* | Cl | >200 |
| **19** | H | Me | Ir | Cp* | Cl | >200 |
| **20** | 4-Me | Me | Ir | Cp* | Cl | 140 ± 40 |
| **21** | H | Ph | Ir | Cp* | I | 52 ± 2 |
| **22** | H | Me | Ir | Cp* | I | 53 ± 4 |
| **25** | 4-Me | Me | Rh | Cp* | Cl | 135 ± 17 |
| Cisplatin | - | - | - | - | - | 0.80 ± 0.01 |

## Cytotoxicity Studies

The toxicity of each complex was assessed against non-small cell lung carcinoma H460 cells. Each complex was incubated with H460 cells for 96 h at concentrations ranging from 0.1 to 200 μM (aqueous media containing 0.1% DMSO) and $IC_{50}$ values were measured using the MTT assay (see ESI† for details). The solubility of complexes at these concentrations was assessed to ensure the compounds are fully dissolved (see ESI† for details). Selected results are shown in Table 2 and represent the mean value for data from at least three experiments. All Ru complexes incorporating chloride ligands are non-toxic up to 200 μM. The most cytotoxic species are the iridium-Cp* complexes **21** and **22**, each with $IC_{50}$ values of 50 ± 5 μM, respectively. The presence of the iodide ligand appears to play an important role in the observed toxicity, as the analogous chloride complexes, **18** and **19**, gave $IC_{50}$ values >200 μM. Comparing complexes **21** (P-phenyl) and **22** (P-methyl), it would appear that the phosphorus-R group has little influence upon the toxicity. However, this is not the case when comparing the Ru-p-cymene complexes **10** and **11**, for which the P-phenyl analogue has significantly greater cytotoxicity than the P-methyl complex. A comparison with cisplatin ($IC_{50}$ = 0.80 ± 0.01 under the experimental conditions), shows that in general this class of complexes have low cytotoxicity. While ineffective as cytotoxic agents, this feature may bode well for uses in applications such as enzyme inhibitors.

A general feature within this series is that the complexes incorporating monodentate iodide ligands have higher toxicities than the corresponding chloride complexes. The extent of hydrolysis of the iodide complexes is less than that of the chloride complexes, leading to the conclusion that a mechanism of action involving hydrolysis and DNA binding, as is often proposed for piano stool metal complexes, may not be the main mechanism of action operating for this series of complexes. Whatever the mechanism, the observation of higher toxicity for iodide complexes is consistent with previously published reports[12,30] for both Ru- and Os-based anticancer complexes. Studies are ongoing to elucidate a potential mechanism of action for these species.

## Binding Studies

In general, the Ru complexes herein have $IC_{50}$ values greater than 200 μM. In an attempt to understand this low cytotoxicity, binding studies were carried out with several biomolecules. Addition of

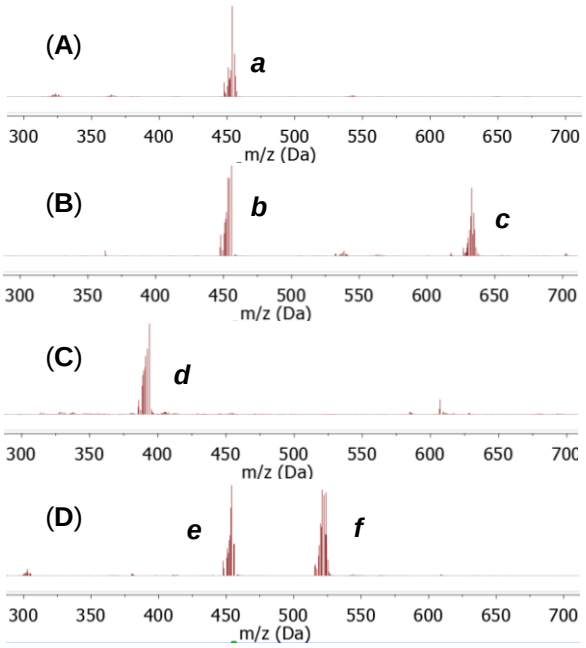


**Fig 6** Mass Spectra for complex **1a** in the presence of (A) L-alanine, (B) 9-ethylguanine, (C) L-histidine and (D) imidazole. Peaks labelled ***a*** **–** ***f*** correlate to peaks in Table 3.

$AgNO_3$ to complex **1** dissolved in $D_2O$, followed by filtration of the resulting AgCl precipitate, gave the aqua adduct, **1a**. Mass spectrometry and NMR spectroscopy ($^1H$ and $^{31}P$) were used to identify the presence and extent of biomolecule binding after addition of one and two equivalents of biomolecule to **1a**, at 1 h and 16 h time-points (Figure 6 and Table 3). The biomolecules selected for investigation were L-alanine (L-Ala), L-threonine (L-Thr), L-histidine (L-His), imidazole and 9-ethylguanine (9-EtG). No evidence for binding between **1a** and 1 equivalent of amino acids L-Ala and L-Thr was observed after 1 h. In contrast, addition of 1 equivalent of 9-EtG led to a peak in the mass spectrum corresponding to the 9-EtG adduct of **1a**, following loss of $H_2O$. $^1H$-NMR analysis indicated the formation of a bond between Ru and N7 on 9-EtG, with around 50% bound complex in solution. This mode of binding is consistent with previous reports that have proposed a mechanism of action for the anticancer behaviour of Ru complexes to involve DNA binding, leading to apoptosis.[16]

Upon addition of 1 equivalent of L-His, an adduct was observed, consistent with replacement of $H_2O$ for L-His, binding though an imidazole N. When the sample was subjected to a second equivalent of L-His and left to equilibrate over 16 h, a species formed in which the pyridylphosphinate ligand is displaced and the L-His binds $\kappa^3$ (Figure 7). The observed Ru–(L-His) complex, **1c**, is known to be non-cytotoxic[31] and its formation presents a potential explanation of the low cytotoxicity of Ru chloride complexes described in this report. It follows that the higher cytotoxicity of the iodide-complexes, **10**, **21** and **22**, is due to the metal–iodide bond being less labile towards aquation and therefore less likely to undergo decomplexation by chelating biomolecules. It should be noted that the only tested biomolecule able to displace the pyridylphosphinate ligand was L-His. Addition of 2 equivalents of imidazole (16 h) leads to 1 : 1 adduct formation, with loss of $H_2O$, but no ligand displacement. The cytotoxicity of the displaced ligand of complex **1** (shown in Fig 7A) was assessed using the MTT assay and found to by non-cytotoxic up to 200 µM. In future studies it may be possible to tune the lability of pyridylphosphinate ligands,

**Table 3** Proposed species that give rise to mass peaks in Figure 6, upon addition of selected biomolecules. Tabulated *m/z* values ***a*** **–** ***f*** correspond to mass peaks in Figure 6.

| Biomolecule | *m/z* | Species |
|---|---|---|
| L-Ala | ***a***: 454.3 | **[1a – $H_2O$]$^+$** 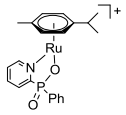 |
| L-Thr | 454.6 | **[1a – $H_2O$]$^+$** |
| 9-EtG | ***b***: 453.8 | **[1a – $H_2O$]$^+$** |
| | ***c***: 632.9 | **1b** 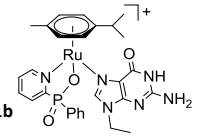 |
| L-His | ***d***: 390.6 | **1c** 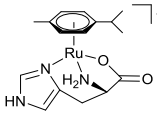 |
| Imidazole | ***e***: 454.0 | **[1a – $H_2O$]$^+$** |
| | ***f***: 522.4 | **1d** 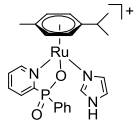 |

so that the complexes remain intact in the high chloride concentration of the extracellular medium but are able to release some useful payload within the cell where the chloride concentration is lower.

## Conclusions

A series of 25 new piano-stool pyridylphosphinate complexes has been synthesised, characterised and assessed in biologically-relevant systems. The properties of the complexes depend upon their various components – metal ion, arene, pyridyl substituent and P–alkyl group – which can be varied with relative ease. Aqueous solubility and stability is good. Ru–Cl complexes are non-toxic up to 200 µM, which bodes well for their use as a scaffold for metal-based enzyme inhibitors. Ir–I complexes are more toxic to cells, so may have the potential to act as anticancer agents,

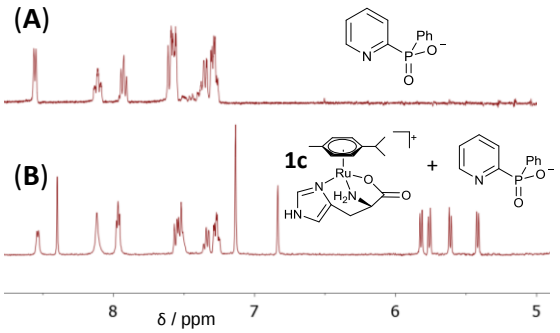


**Fig 7** $^1H$-NMR spectra ($D_2O$ : $CD_3OD$ 9:1, 298 K, 400 MHz) of (A) uncomplexed pyridylphosphinate ligand and (B) products of addition of 2 equivalents of L-His to complex **1a**, showing the decomplexation of the pyridylphosphinate ligand and the formation of L-His complex, **1c**

although toxicity remains low compared to cisplatin. It was discovered that decomplexation of the ligand from complex **1** occurs in the presence of excess L-His, following hydrolysis of the Ru–Cl bond. This has the potential to be exploited in the form of complexes that deliver and release useful payloads to the cell. The rate of aquation and the p$K_a$ of the resulting aqua species can be tuned by varying the pyridyl substiuent and the judicious choice of metal–halide combination. Studies are ongoing to investigate the cell uptake, localisation and any potential antimetastatic behaviour of these exciting new complexes and to exploit the lability of the phenylphosphinate Ru bond to design responsive biologically active complexes.

## Acknowledgements

We thank Durham University and the EPSRC for funding.

## Notes and references


1 (a) S. W. Botchway, M. Charnley, J. W. Haycock, A. W. Parker, D. L. Rochester, J. A. Weinstein and J. A. G. Williams, *Proc. Natl. Acad. Sci. U. S. A.*, 2008, **105**, 16071; (b) D. Lloyd, M. P. Coogan and S. J. A. Pope, *Rev. Fluoresc.*, 2012, vol. 2010, 15.

2 (a) M. Dorr and E. Meggers, *Curr. Opin. Chem. Biol.*, 2014, **19**, 76; (b) D. Hu, Y. Liu, Y.-T. Lai, K.-C. Tong, Y.-M. Fung, C.-N. Lok and C.-M. Che, *Angew. Chem. Int. Ed.*, 2016, **55**, 1387

3 (a) F. E. Poynton, J. P. Hall, P. M. Keane, C. Schwarz, I. V. Sazanovich, M. Towrie, T. Gunnlaugsson, C. J. Cardin, D. J. Cardin, S. J. Quinn, C. Long, J. M. Kelly, *Chem. Sci.*, 2016, **7**, 3075; (b) K.K.W. Lo, T. K. M. Lee, J. S. Y. Lau, W. L. Poon and S. H. Cheng, *Inorg. Chem.*, 2008, **47**, 200; (c) K. K.-W. Lo, *Acc. Chem. Res.*, 2015, **48**, 2985.

4 For recent reviews of metal-based anticancer agents see (a) G. Gasser, I. Ott and N. Metzler-Nolte, *J. Med. Chem.*, 2011, **54**, 3; (b) I. Ott and R. Gust, *Arch. Pharm.*, 2007, **340**, 117; (c) S. Medici, M. Peana, V. M. Nurchi, J. I. Lachowicz, G. Crisponi and M. A. Zoroddu, *Coord. Chem. Rev.*, 2015, 329; (d) N. Muhammad and Z. Guo, *Curr. Opin. Chem. Biol.*, 2014, **19**, 144.

5 (a) B. Rosenberg, L. van Camp and T. Krigas, *Nature*, 1965, **205**, 698; (b) Y. Kidani, K. Inagaki, M. Iigo, A. Hoshi and K. Kuretani, *J. Med. Chem.*, 1978, **21**, 1315; (c) K. R. Harrap, *Cancer Treat. Rev.*, 1985, **12**, 21.

6 (a) H. Matsushima, K. Yonemura, K. Ohishi and A. Hishida, *J. Lab. Clin. Med.*, 1998, **131**, 518; (b) N.E. Madias and J. T. Harrington, *Am. J. Med.*, 1978, **65**, 307.

7 (a) M. Kartalou and J. M. Essigmann, *Mutat. Res.*, 2001, **478**, 23; (b) K. J. Mellish, L. R. Kelland and K. R. Harrap, *Br. J. Cancer*, 1993, **68**, 240.

8 A. A. Nazarov, C. G. Hartinger and P. J. Dyson, *J. Organometal. Chem.*, 2014, **751**, 251.

9 (a) R. E. Morris, R. E. Aird, P. del Socorro-Murdoch, H. Chen, J. Cummings, N. D. Hughes, S. Parsons, A. Parkin, G. Boyd, D. I. Jodrell and P. J. Sadler, *J. Med. Chem.*, 2001, **44**, 3616; (b) M. Pernot, T. Bastogne, N. P. E. Barry, B. Therrien, G. Koellensperger, S. Hann, V. Reshetov and M. Barberi-Heyob, *J. Photoch. Photobio. B*, 2012, **117**, 80; (c) A. A. Nazarov, S. M. Meier, O. Zava, Y. N. Nosova, E. R. Milaeva, C. G. Hartinger and P. J. Dyson, *Dalton Trans.*, 2015, **44**, 3614; (d) S. M. Meier, M. Hanif, Z. Adhireksan, V. Pichler, M. Novak, E. Jirkovsky, M. A. Jakupec, V. B. Arion, C. A. Davey, B. K. Keppler and C. G. Hartinger, *Chem. Sci.*, 2013, **4**, 1837; (e) B. S. Murray, L. Menin, R. Scopelliti and P. J. Dyson, *Chem. Sci.*, 2014, **5**, 2536.

10 (a) C. Scolaro, A. Bergamo, L. Brescacin, R. Delfino, M. Cocchietto, G. Laurenczy, T. J. Geldbach, G. Sava and P. J. Dyson, *J. Med. Chem.*, 2005**, 48**, 4161; (b) A. Weiss, R. H. Berndsen, M. Dubois, C. Müller, R. Schibli, A. W. Griffioen, P. J. Dyson and P. Nowak-Sliwinska, *Chem. Sci.*, 2014, **5**, 4742; (c) X. Meng, M. L. Leyva, M. Jenny, I. Gross, S. Benosman, B. Fricker, S. Harlepp, P. Hébraud, A. Boos, P. Wlosik, P. Bischoff, C. Sirlin, M. Pfeffer, J. P. Loeffler, C. Gaiddon, *Cancer Res.*, 2009, **69**, 5458.

11 (a) O. Novakova, H. Chen, O. Vrana, A. Rodger, P. J. Sadler and V. Brabec, *Biochemistry*, 2003, **42**, 11544; (b) R. E. Morris, R. E. Aird, P. del Socorro-Murdoch, H. Chen, J. Cummings, N. D. Hughes, S. Parsons, A. Parkin, G. Boyd, D. I. Jodrell and P. J. Sadler, *J. Med. Chem.*, 2001, **44**, 3616.

12 S. H. van Rijt, I. Romero-Canelón, Y. Fu, S. D. Shnyder and P. J. Sadler, *Metallomics*, 2014, **6**, 1014.

13 K. D. Camm, A. El-Sokkary, A. L. Gott, P. G. Stockley, T. Belyaevab and P. C. McGowan, *Dalton Trans.*, 2009, **48**, 10914.

14 A. F. A. Peacock, S. Parsons and P. J. Sadler, *J. Am. Chem. Soc.*, 2007, **129**, 3348.

15 (a) Z. Liu, A. Habtemariam, A. M. Pizarro, S. A. Fletcher, A. Kisova, O. Vrana, L. Salassa, P. C. A. Bruijnincx, G. J. Clarkson, V. Brabec and P. J. Sadler, *J. Med. Chem.*, 2011, **54**, 3011; (b) Z. Liu, I. Romero-Canelón, B. Qamar, J. M. Hearn, A. Habtemariam, N. P. E. Berry, A. M. Pizarro, G. J. Clarkson and P. J. Sadler, *Angew. Chem. Int. Ed.*, 2014, **53**, 3941; (c) Z. Liu and P. J. Sadler, *Acc. Chem. Res.*, 2014, **47**, 1174; (d) M. Grasa, B. Therrien, G. Süss-Fink, A. Casini, F. Edafe and P. J. Dyson, *J. Organometal. Chem.*, 2010, **695**, 1119; (e) L. C. Sudding, R. Payne, P. Govender, F. Edafe, C. M. Clavel, P. J. Dyson, B. Therrien and G. S. Smith, *J. Organometal. Chem.*, 2014, **774**, 79.

16 H. Chen, J. A. Parkinson, S. Parsons, R. A. Coxall, R. O. Gould and P. J. Sadler, *J. Am. Chem. Soc.*, 2002, 124, 3064.

17 Z. Adhireksan, G. E. Davey, P. Campomanes, M. Groessl, C. M. Clavel, H. Yu, A. A. Nazarov, C. Hui Fang Yeo, W. Han Ang, P. Dröge, U. Rothlisberger, P. J. Dyson and C. A. Davey, Nature Commun., 2014, **5**, 3462.

18 (a) A. de Almeida, B. L. Oliveira, J. D. G. Correia, G. Soveral and A. Casini, *Coord. Chem. Rev.*, 2013, **257**, 2689; (b) L. Feng, Y. Geisselbrecht, S. Blanck, A. Wilbuer, G. E. Atilla-Gokcumen, P. Filippakopoulos, K. Kräling, M. A. Celik, K. Harms, J. Maksimoska, R. Marmorstein, G. Frenking, S. Knapp, L.-O. Essen and E. Meggers, *J. Am. Chem. Soc.*, 2011, **133**, 5976; (c) E. Meggers, G. E. Atilla-Gokcumen, K. Gründler, C. Frias, A. Prokop, *Dalton Trans.*, 2009, 10882.

19 (a) I. Romero-Canelón and P. J. Sadler, *Inorg. Chem.*, 2013, **52**, 12276; (b) K. Suntharalingam, Y. Song and S. J. Lippard, *Chem. Commun.*, 2014, **50**, 2465.

20 (a) S. J. Butler, M. Delbianco, L. Lamarque, B. K. McMahon, E. R. Neil, R. Pal, D. Parker, J. W. Walton and J. M. Zwier, *Dalton Trans.*, 2015, **44**, 4791; (b) M. Soulié, F. Latzko, E. Bourrier, V. Placide, S. J. Butler, R. Pal, J. W. Walton, P. L. Baldeck, B. Le Guennic, C. Andraud, J. M. Zwier, L. Lamarque, D. Parker and O. Maury, *Chem. Eur. J.*, 2014, **20**, 8636; (c) A. J. Palmer, S. H. Ford, S. J. Butler, T. J. Hawkins, P. J. Hussey, R. Pal, J. W. Walton and D. Parker, *RSC Adv.*, 2014, **4**, 9356.

21 Examples of enantiomerically pure anticancer metal complexes include (a) G. E. Atilla-Gokcumen, L. Di Costanzo and E. Meggers, *J. Biol. Inorg. Chem.*, 2011, **16**, 45; (b) E. Menéndez-Pedregal, Á. Manteca, J. Sánchez, J. Díez, M. P. Gamasa and E. Lastra, *Eur. J. Inorg. Chem.*, 2015, 1424.

22 (a) J. W. Walton, L. Di Bari, D. Parker, G. Pescitelli, H. Puschmann and D. S. Yufit, *Chem. Commun.*, 2011, **47**, 12289; (b) J. W. Walton, R. Carr, N. H. Evans, A. M. Funk, A. M. Kenwright, D. Parker, D. S. Yufit, M. Botta, S. De Pinto and K.-L. Wong, *Inorg. Chem.*, 2012, **51**, 8042.


 

23 (a) J. W. Walton, A. Bourdolle, S. J. Butler, M. Soulie, M. Delbianco, B. K. McMahon, R. Pal, H. Puschmann, J. M. Zwier, L. Lamarque, O. Maury, C. Andraud and D. Parker, *Chem. Commun.*, 2013, **49**, 1600; (b) S. J. Butler, R. Pal, B. K. McMahon, D. Parker and J. W. Walton, *Chem. Eur. J.*, 2013, **19**, 9511.

24 C. Gossens, I. Tavernelli and U. Rothlisberger, *J. Phys. Chem. A*, 2009, **113**, 11888.

25 S. H. van Rijt, A. F. A. Peacock, R. D. L. Johnstone, S. Parsons and P. J. Sadler, *Inorg. Chem.*, 2009, **48**, 1753.

26 A. Krezel and W. J. Bal, *Inorg. Biochem.*, 2004, **98**, 161.

27 P. Moore, in Inorganic Reaction Mechanisms Vol. 4, ed. A. McAuley, CRC Press, Boca Raton, 1988, pp. 129.

28 (a) M. Melchart, A. Habtemariam, S, Parsons, S. A. Moggach, P. J. Sadler, *Inorg. Chim. Acta.*, 2006, **359**, 3020; (b) W. Kandioller, C. Hartinger, A. A. Nazarov, M. L. Kuznetsov, R. John, C. Bartel, M. A. Jakupec, V. B. Arion, B. K. Keppler, *Organometallics*, 2009, **28**, 4249.

29 Q. Q. Li, G. Wang, F. Huang, J. M. Li, C. F. Cuff and E. Reed, *Med. Oncol.*, 2013, **30**, 488.

30 I. Romero-Canelón, L. Salassa and P. J. Sadler, *J. Med. Chem.*, 2013, **56**, 1291.

31 T. G. Scrase, M. J. O'Neill, A. J. Peel, P. W. Senior, P. D. Matthews, H. Shi, S. R. Boss and P. D. Barker, *Inorg. Chem.*, 2015, **54**, 3118.